



LAWRENCE  
LIVERMORE  
NATIONAL  
LABORATORY

# The study of X-ray M-shell spectra of W ions from the LLNL Electron Beam Ion Trap

P. Neill, C. Harris, A. S. Shlyaptseva, S. Hamasha, S. Hansen, P. Beiersdorfer, U. I. Safronova

December 15, 2003

Canadian Journal of Physics

## **Disclaimer**

---

This document was prepared as an account of work sponsored by an agency of the United States Government. Neither the United States Government nor the University of California nor any of their employees, makes any warranty, express or implied, or assumes any legal liability or responsibility for the accuracy, completeness, or usefulness of any information, apparatus, product, or process disclosed, or represents that its use would not infringe privately owned rights. Reference herein to any specific commercial product, process, or service by trade name, trademark, manufacturer, or otherwise, does not necessarily constitute or imply its endorsement, recommendation, or favoring by the United States Government or the University of California. The views and opinions of authors expressed herein do not necessarily state or reflect those of the United States Government or the University of California, and shall not be used for advertising or product endorsement purposes.

**The study of X-ray M-shell spectra of W ions  
from the LLNL Electron Beam Ion Trap**

P. Neill, C. Harris, A. S. Shlyaptseva, S. Hamasha, S. Hansen

*Physics Department/220, University of Nevada, Reno, NV 89557*

P. Beiersdorfer

*Lawrence Livermore National Laboratory, Livermore, CA 94550*

U. I. Safronova

*Department of Physics, University of Notre Dame, IN 46556*

**Abstract**

M-shell spectra of W ions have been produced at the Livermore EBIT-II electron beam ion trap at different energies of the electron beam. A survey has been performed for 2.4 keV, 2.8 keV, 3.6 keV and for steps in energy of 100 eV over the 3.9-4.6 keV energy range. The analysis of 11 W spectra has shown the presence of a wide variety of ionization stages from Se-like to Cr-like W; the appearances of these ionization stages correlate well with the energy of their production. The present paper focuses on the identification of 63 experimental features of W ions in a spectral region from 5 to 6 Å using calculations with inclusion of all ionization stages matching this spectral region. The majority of lines in all spectra have been identified and assigned to the  $4f \rightarrow 3d$  and  $4d \rightarrow 3p$  transitions. This is the first work that lists a comprehensive identification of so many resolved spectral features of M-shell transitions in W ions recorded in such detail in the laboratory.

## I. Introduction.

Tungsten wire explosions are being very intensively studied at Sandia National Laboratories. Results of tungsten wire-array Z-pinch experiments and modeling have been published elsewhere [1,2]. High-resolution x-ray spectral data have been accumulated in tungsten experiments on Z [3], which require a development of appropriate theoretical modeling. The study of x-ray M-shell spectra of W ions produced by high-temperature plasmas is a very complicated problem because of the simultaneous contributions from numerous ionization stages. For example, the majority of line emissions in the spectral region from 5 to 6 Å are composed of hundreds of  $4l' \rightarrow 3l$  transitions and more than ten ionization stages. Identification of this spectral region is a complex problem even for low-density Tokamak plasmas [4]. To our best knowledge, the first x-ray M-shell spectra of W have been produced by high-density exploded-wire plasmas more than 25 years ago. The achieved precision of the measurement of the transitions energies at the  $\pm 10$  eV level was sufficient to identify three Ni-like W lines and determine ionization states from Zn-like to Fe-like W, but was not enough for the purely spectroscopic tabulations [5]. The precision of the measurement of the  $4l' \rightarrow 3l$  Ni-like W transitions was substantially improved three years later in the identification of Hf XLV, Ta XLVI, W XLVII, and Re XLVIII ions produced by laser plasmas [6]. The following paper on laser plasma M-shell heavy ions [7] concentrated on  $4p \rightarrow 3d$  transitions in Co- and Cu-like W and Tm because their separation is greater than for the  $4f \rightarrow 3d$  spectral lines. The extended analysis of the X-ray spectra of laser-irradiated W included  $nf \rightarrow 3d$  ( $n=5$  through 9),  $nd \rightarrow 3p$  ( $n=4$  through 6) and  $np \rightarrow 3s$  ( $n=4,5$ ) transitions [8].

Recently, electron-beam ion-trap EUV spectra of W ions have been studied at the Berlin [9] and Livermore [10] electron beam ion traps. In electron beam ion trap experiments, the complicated M-shell spectrum can be decomposed in various spectra formed by the contribution of only few ionization stages allowing for the possibility to unravel the tungsten M-shell emission. These capabilities have been used to identify the complex EUV emission [9,10] and x-ray emission of W in the present paper. Specifically, we present an analysis of eleven x-ray M-shell spectra produced at different energies of the electron beam. These spectra are formed by a wide variety of ionization stages of W ions, from Se- to Cr-like W. The important feature of these spectra is that every spectrum includes prominent lines from only a few ionization stages. The variation in intensities with

beam energy allows these lines to be uniquely identified with particular charge states. Some atomic data and spectral intensities for Co-like to Rb-like W ions have been previously calculated for high-temperature, low-density plasma for a broad spectral range  $0 < \lambda < 20 \text{ \AA}$  [11]. In the present paper, we focus on the identification of experimental spectral features of W ions in a spectral range from  $5 \text{ \AA}$  to  $6 \text{ \AA}$  using the calculations which include all ionization states matching this spectral region.

## II. Experimental M-shell spectra in the spectral region from $5 \text{ \AA}$ to $6 \text{ \AA}$ .

An M-shell survey of W ions was performed at Lawrence Livermore National Laboratory using the EBIT-II electron beam ion trap. The trapped W ions reach a charge-state limit when the electron beam energy is below the energy required to produce the next higher charge state. For this survey, steady-state electron beam energies were  $2.4 \text{ keV}$ ,  $2.8 \text{ keV}$ ,  $3.6 \text{ keV}$  and in steps of  $100 \text{ eV}$  over the  $3.9\text{-}4.6 \text{ keV}$  energy range. The eleven experimental spectra, shown in Figs. 1-5, are each dominated by one or a few charge states, and exhibit the shift in charge balance toward higher charge states with increasing beam energy. These spectra were recorded by a wide-band, high-resolution soft x-ray spectrometer [12] with a PET(002) crystal. The resolution was  $\lambda/\Delta\lambda=2200$  and the detected spectral range was from  $5 \text{ \AA}$  to  $5.94 \text{ \AA}$ .

Two prominent phosphorus lines,  $\text{Ly}_\alpha$  ( $\lambda = 5.3814 \text{ \AA}$ ) and the He-like resonance line w ( $\lambda = 5.7600 \text{ \AA}$ ), were used directly for wavelength calibration of the spectra taken at  $2.4 \text{ keV}$  and  $3.9 \text{ keV}$ . The wavelength scale was determined using a Gaussian profile fitting function followed by a correction to account for the intersection of the dispersion plane with the flat face of the position-sensitive proportional counter. As noted in previous measurements utilizing similar detectors [13], the line positions at the single-wire proportional counter were observed to shift physically by small amounts from one spectrum to the next. There were two components to these small shifts. The most pronounced was a seemingly random systematic shift of the entire spectrum toward higher or lower detector channels. Smaller random shifts displaced individual lines relative to the others. The systematic shifts may have been caused by mechanical vibration or thermal expansion and contraction of the spectrometer, but these mechanisms fail to explain the random line-to-line shifts within spectra. As there was about  $1 \text{ m\AA}$  of systematic shift from spectrum to spectrum, we used the prominent Ni-like Ni1 and Ni2 lines as a secondary standard. These Ni-like lines are present in all the spectra except

that taken at beam energy 2.4 keV, and were used to calibrate the wavelength scale for the 2.8keV - 4.6 keV spectra. The line-to-line random shifts are responsible for a relative wavelength uncertainty of 0.3 mÅ.

The eleven experimental spectra were accumulated for varying periods, so while the relative line intensities in a particular spectrum are meaningful, intensity comparisons between spectra are not. Line intensity as shown in the figures is measured in counts (per wavelength bin), while in the tables experimental intensity is the integrated counts under the fitted Gaussian profile for that line. Statistical uncertainty in the experimental intensity is calculated as the square root of the integrated counts for unblended lines. This suggests that the error bars should range from 24% for the least intense line down to less than 1% for the most intense. However, for this survey experiment, no intensity correction was made for polarization effects of the crystal or for the response function of the 1 micrometer lexan window of the wide-band spectrometer.

### **III. Modeling of M-shell W spectra in the spectral region from 5 to 6Å.**

All together we have studied eleven spectra recorded in the spectral region from 5 to 6Å, which are presented in Figs. 1-5. The observed transitions are  $4l' \rightarrow 3l$  transitions from Se-like through Cr-like W. For all eleven spectra the brightest lines are lines due to  $4f_{5/2} \rightarrow 3d_{3/2}$  transitions (Group 1). The most prominent lines in the majority of spectra are Ni-like ion lines. Group 2 is made up of  $4f_{7/2} \rightarrow 3d_{5/2}$  transitions, these are less intense and have longer wavelengths than Group 1. Group 3, formed by  $4d \rightarrow 3p$  transitions, is characterized by less intense lines with shorter wavelengths than Groups 1 and 2. Ga-like lines from Group 1 (Ga1) dominate the 2.4 keV spectrum, whereas a Ni-like line (Ni1) dominates in the other ten spectra. The most intense of the Cu-like line peaks (Cu1) is observed in all spectra. Zn-like line features are very intense in the 2.4 keV spectra, then decrease in relative intensities through the 4.0 keV spectrum. Co-like lines appear in the 3.9 keV spectrum and are very intense in the 4.2-4.6 keV spectra. Mn-like and Fe-like line features become prominent in the 4.5 keV and 4.6 keV spectra.

To identify the x-ray M-shell spectra of W ions, the necessary atomic data have been calculated and a collisional-radiative atomic kinetic model has been developed. Atomic data of all

needed isoelectronic sequences matching this spectrum were calculated using the MCHF code developed by Cowan [14]. Also, wavelengths and transition probabilities for Ni-like W lines were calculated using the fully relativistic many-body code (RMBPT code) [15]. Table 1 presents wavelengths and weighted transition rates for transitions from ten excited  $J=1$  states to the ground state in Ni-like W. Theoretical data obtained by using the RMBPT and Cowan codes are compared with experimental spectra of this paper and the previous experimental work published in [6,8]. The accuracy of measured wavelengths was 0.005 Å in [6] and 0.002 Å in [8]. The experimental wavelengths of four Ni-like lines (7, 11, 46, and 61) from this paper are averaged values over all measurements listed in Table 2.

The second-order RMBPT calculations implemented here for Ni-like ions start from a  $1s^2 2s^2 2p^6 3s^2 3p^6 3d^{10}$  Dirac-Fock potential [15]. All possible  $3l$  holes and  $4l$  particles forming 56 odd-parity and 50 even-parity  $3l^{-1}4l'$  ( $J$ ) states have been considered. In general, theoretical results are in a good agreement with experiment, however, RMBPT wavelengths agree much better with experimental measurements than the Cowan wavelengths. For example, for the transitions from the  $3p_{3/2}4d_{5/2}$  and  $3p_{3/2}4d_{3/2}$  levels, RMBPT calculations give  $\lambda_{\text{RMBPT}}=5.201$  Å and  $\lambda_{\text{RMBPT}}=5.255$  Å, which are much closer to the experimental measurements  $\lambda_{\text{exp}}=5.1963$  Å and  $\lambda_{\text{exp}}=5.2509$  Å than the Cowan calculations ( $\lambda_{\text{Cowan}}=5.218$  Å and  $\lambda_{\text{Cowan}}=5.272$  Å), respectively. On the other hand, it should be noted that the atomic structure Cowan code produces results which are generally in good agreement with experimental energies by scaling the electrostatic Slater parameters to include the correlation effects. The scaling factor of 0.85 and LS coupling were employed in the Cowan code calculations. Also, contributions from many configurations for each isoelectronic sequence were taken into account in calculations of atomic characteristics by Cowan code. For example, for Cu-like ions, fourteen even and twelve odd parity configurations of excited singly and doubly excited states were included in the calculations. To calculate synthetic M-shell spectra of W, the most intense 542 lines of Cr-like, 345 lines of Mn-like, 461 lines of Fe-like, 148 lines of Co-like, 47 lines of Ni-like, 368 lines of Cu-like, 1213 lines of Zn-like, 522 lines of Ga-like, 370 lines of Ge-like, 147 lines of As-like, and 100 lines of Se-like W ions were included.

The collisional-radiative atomic kinetic model includes the ground states of every ionization stage of W from the bare ion with no electrons to neutral W with 74 electrons. Ionization potentials were taken from published tables [11,16]. Detailed atomic structure is included for ionization stages

from Cr-like to Se-like W. Each fine structure state is linked to other states within its ionization stage via collisional excitation, collisional de-excitation, and radiative decay. All states of ions are linked via collisional ionization, three-body recombination, and radiative recombination. The modified Van Regemorter [17] formula is used to calculate the excitation cross sections of optically allowed transitions. A modified Lotz formula [18] is employed to calculate collisional ionization cross sections. Radiative recombination cross sections are calculated with Kramer's approximation [19]. The electron distribution function used in the model had a Gaussian form centered at the indicated energy of the electron beam with a FWHM=50 eV in agreement with typical distributions measured on EBIT-II [20].

Synthetic spectra calculated using the kinetic model with lines broadened with Doppler profiles for each of eleven ionization stages are shown in Figs. 6 (a,b,c). Specifically, the synthetic spectra of Se- to Ga-like W ions are presented in Fig. 6a. The spectra of Se- to Ge-like W exhibit only Group 1 peaks, whereas the spectrum of Ga-like W ions shows peaks corresponding to all three Groups 1-3. The synthetic spectra of Zn- to Co-like W ions are presented in Fig. 6b. The spectra of Ni- to Co-like W ions consist of peaks due to Groups 1-3. The synthetic spectra of Fe- to Cr-like W ions are presented in Fig. 6c. The spectrum of Fe-like W ions consists of peaks due to Groups 1-3, whereas the spectra from Mn- and Cr-like W ions include two peaks due to Groups 1 and 2. To identify experimental line features, the wavelengths and intensities of the most intense peaks within the three groups of transitions for each ionization stage have been compared with experimental wavelengths and relative intensities. Table 2 lists identification of 63 M-shell line features from eleven spectra of W ions. In general, experimental observations agree well with theoretical predictions from this paper and from Ref. [11]. Specifically, the spectra produced at 2.4 keV and 2.8 keV (Fig. 1) are rich with ions of ionization stages lower than Ni-like: from Se-like to Cu-like W. The spectrum produced at 2.4 keV is the only spectrum among eleven spectra where no Ni-like ion lines are observed. The synthetic spectrum of Ga-like W reproduces well the most intense lines for this spectral feature and beam energy (Fig. 7a). The spectra produced at 3.6 keV and 3.9 keV (Fig. 2) and at 4.0 keV, 4.1 keV, and 4.2 keV (Fig. 3) are dominated by Ni-like W lines. In the spectrum produced at 3.6 keV we still observe the lower ionization stages of Cu- and Zn-like W, whereas in the spectra produced at 4.1 keV-4.2 keV the ionization stages higher than Ni-like, specifically, Co-like W, appear. This correlates well with the jump in the ionization potential from 2430 eV (for Cu-like W) to 4065

eV (for Ni-like W) and explains why the spectra produced at 3.6 keV-4.2 keV include the least number of lines from all spectra considered. The spectra produced at 4.3-4.6 keV (Figs. 4-5) are rich with higher than Ni-like ionization stages: Co-like, Fe-like, Mn-like, and Cr-like W. The spectrum produced at the highest energy, 4.6 keV, includes the most lines. Also, the maximum number of identified line peaks within a given isoelectronic sequence is 15 for Fe-like W. The synthetic spectrum of Fe-like W reproduces well the most relevant spectral features in Fig. 7b.

#### **IV. Conclusion.**

The survey of eleven W spectra has shown the presence of wide variety of ionization stages from Se-like to Cr-like W: the appearance of these ionization stages correlates well with the energy of their production. The majority of lines in all spectra have been identified and assigned to the  $4f \rightarrow 3d$  and the  $4d \rightarrow 3p$  transitions. The Ni-like ions dominate in most spectra. The high resolution of these spectra and the ability to create only a few ionization stages during the spectrum production allows performing an analysis of the M-shell spectra that can be not done with other sources than an electron beam ion trap. The synthetic spectra calculated using a developed kinetic model reproduce well the most intense spectral features in all eleven experimental spectra. This work lists for the first time a comprehensive identification of so many resolved x-ray spectral features of M-shell transitions of W recorded with such detail in the laboratory.

This study is very important in development of M-shell diagnostics of high density and temperature z-pinch plasmas, for example, plasmas of tungsten wire explosions and x-pinches. M-shell spectra of such plasmas include simultaneous contributions from numerous ionization states. Also, if time and spatial integration is employed to collect the spectra, then it in addition will complicate the analysis. Nevertheless, the kinetic model used in this paper predicts that the most intense spectral features in z-pinch plasmas are Ni-, Cu-, and Co-like W features studied in detail in this work.

## Acknowledgements

The present work was supported by the DOE-NNSA/NV Cooperative Agreement DE-FC08-01NV14050 and Lawrence Livermore National Laboratory under contract B520743. Work at UC, Lawrence Livermore National Laboratory was performed under the auspices of the Department of Energy under Contract No. W-7405-Eng-48.

## References

1. R.B. Spielman, C. Deeney, G.A. Chandler *et al.*, *Phys. Plas.* **5**, 2105 (1998).
2. C. Deeney, C.A. Coverdale, M. Douglas *et al.*, *Phys. Plas.* **6**, 3576 (1999).
3. J. Bailey, D. Cohen, G.A. Chandler, M.E. Cuneo, M.E. Foord *et al.*, *JQSRT* **71**, 157 (2001).
4. R. Neu, K.B. Fournier, D. Schlögl, J. Rice, *J. Phys. B* **30**, 5057 (1997).
5. P.G. Burkhalter, C.M. Dozier, and D.J. Nagel, *Phys. Rev. A* **15**, 700 (1977).
6. A. Zigler, H. Zmore, N. Spector, M. Klapish, J.L. Schwob, A. Bar-Shalom, *J. Opt. Soc. Am.* **70**, 129 (1980).
7. M. Klapish, P. Mandelbaum, A. Barshalom, J.L. Schwob, A. Zigler, S. Jackel, *J. Opt. Soc. Am.* **71**, 1276 (1981).
8. N. Tragin, J-P. Geindre, P. Monier *et al.*, *Physica Scripta* **37**, 72 (1988).
9. R. Radtke, C. Biedermann, J.L. Schwob, P. Mandelbaum, and R. Doron, *Phys. Rev. A* **64**, 012720 (2001).
10. S.B. Utter, P. Beiersdorfer, and E. Träbert, *Can. J. Phys.* **80**, 1503 (2002).
11. K.B. Fournier, *ADNDT* **68**, 1 (1998).
12. G.V. Brown, P. Beiersdorfer, K. Widmann, *Rev. Sci. Instr.* **70**, 280 (1999).

13. S. Elliott, P. Beiersdorfer, J. Nilsen, *Physica Scripta* **49**, 556 (1994).
14. R.D. Cowan, *The Theory of Atomic Structure and Spectra* (University of California Press, Berkeley, 1981).
15. U.I. Safronova, W.R. Johnson, and J.R. Albritton, *Phys. Rev. A* **62**, 052505 (2000).
16. T.A. Carlson, C.W. Nestor, N. Wasserman, and J.D. McDowell, *Oak Ridge National Laboratory Report* **4562** (1970).
17. H.V. Regemorter, *Astrophys. J.* **136**, 906 (1962).
18. V.A. Bernshtam, Y. V. Ralchenko, and Y. Maron, *J. Phys. B* **33**, 5025 (2000).
19. V.P. Shevelko, *Atoms and Their Spectroscopic Properties* (Spring-Verlag, Berlin, 1997).
20. P. Beiersdorfer, T.W. Phillips, K.L. Wong, R.E. Marrs, D.A. Vogel, *Phys. Rev. A* **46**, 3812 (1992).

### Figure Captions

Fig. 1. Experimental M-shell spectrum of W ions produced at the energies of the electron beam of 2.4 keV (top) and 2.8 keV (bottom). Intense spectral features are identified with a certain W ion and a certain group of transitions (see text).

Fig. 2. Experimental M-shell spectrum of W ions produced at the energies of the electron beam of 3.6 keV (top) and 3.9 keV (bottom). Intense spectral features are identified with a certain W ion and a certain group of transitions (see text).

Fig. 3. Experimental M-shell spectrum of W ions produced at the energies of the electron beam of 4.0 keV (top), 4.1 keV (middle) and 4.2 keV (bottom) Intense spectral features are identified with a certain W ion and a certain group of transitions (see text).

Fig. 4. Experimental M-shell spectrum of W ions produced at the energies of the electron beam of 4.3 keV (top) and 4.4 keV (bottom). Intense spectral features are identified with a certain W ion and a certain group of transitions (see text).

Fig. 5. Experimental M-shell spectrum of W ions produced at the energies of the electron beam of 4.5 keV (top) and 4.6 keV (bottom). Intense spectral features are identified with a certain W ion and a certain group of transitions (see text).

Fig. 6. Theoretical synthetic spectra of Se- to Ga-like W ions (a), Zn- to Co-like W ions (b), and Fe- to Cr-like W ions (c) calculated using a kinetic code.

Fig. 7. Comparisons of the most intense spectral features in experimental spectra produced at 2.4 keV (top) and 4.6 keV (bottom) with synthetic spectra of Ga-like and Fe-like Ions, respectively.

**Table 1. Wavelengths ( $\lambda$  in Å) and weighted transition rates ( $gA_r$  in  $s^{-1}$ ) in Ni-like W for transitions from odd-parity states with  $J=1$  to the ground state. Theoretical data obtained using RMBPT and Cowan codes are compared with experimental results of the present paper (a) and with the previous experimental results from Ref. [6] (b) and Ref. [8] (c). Numbers in brackets represent powers of 10.**

<i>jj</i> label	<i>LS</i> label	experiment		theory			
		$\lambda_{\text{exp}}$	$\lambda_{\text{exp}}$	$\lambda_{\text{RMBPT}}$	$\lambda_{\text{COWAN}}$	$gA_r^{\text{RMBPT}}$	$gA_r^{\text{COWAN}}$
$3d_{3/2}4p_{1/2}$	$3d4p \ ^3D_1$		7.170 <sup>b</sup>	7.174	7.164	2.00 [13]	1.62 [13]
$3d_{5/2}4p_{3/2}$	$3d4p \ ^1P_1$		7.024 <sup>b</sup>	7.027	7.008	3.82 [13]	3.91 [13]
$3d_{3/2}4p_{3/2}$	$3d4p \ ^3P_1$		6.775 <sup>b</sup>	6.778	6.754	4.20 [12]	5.35 [12]
$3p_{3/2}4s_{1/2}$	$3p4s \ ^1P_1$		6.154 <sup>b</sup>	6.156	6.174	6.65 [13]	5.21 [13]
$3d_{5/2}4f_{5/2}$	$3d4f \ ^3P_1$		5.956 <sup>b</sup>	5.953	5.946	7.24 [11]	3.90 [11]
$3d_{5/2}4f_{7/2}$	$3d4f \ ^3D_1$	5.8665 <sup>a</sup>	5.871 <sup>b</sup>	5.870	5.868	3.54 [14]	4.21 [14]
$3d_{3/2}4f_{5/2}$	$3d4f \ ^1P_1$	5.6900 <sup>a</sup>	5.689 <sup>b</sup>	5.689	5.685	1.12 [15]	1.22 [15]
$3p_{1/2}4s_{1/2}$	$3p4s \ ^3P_1$			5.345	5.324	1.71 [13]	3.05 [13]

$3p_{3/2}4d_{3/2}$	$3p4d$	$^3P_1$	5.2509 <sup>a</sup>	5.255 <sup>c</sup>	5.255	5.272	1.58[13]	1.77[13]
$3p_{3/2}4d_{5/2}$	$3p4d$	$^1P_1$	5.1963 <sup>a</sup>	5.203 <sup>c</sup>	5.201	5.218	2.82[14]	2.55[14]

**Table 2. Identification of lines in M-shell spectra of W produced at different energies of the electron beam from 2.4 to 4.6 keV. Atomic data are calculated using Cowan code and RMBPT code (a).**

Experimental data (wavelengths and intensities) produced at different energies of the electron beam								
N	Ion/ Group	Theor. $\lambda$ (Å)	2.4 keV		2.8 keV		3.6 keV	
			Exp. $\lambda$ (Å)	Int.	Exp. $\lambda$ (Å)	Int.	Exp. $\lambda$ (Å)	Int.
7	Ni3	5.201 <sup>a</sup>			5.1953	297	5.1976	129
8	Cu3	5.230			5.2239	135		
9	Cu3	5.241			5.2331	348		
11	Ni3	5.255			5.2491	88		
12	Zn3	5.280	5.2738	91	5.2705	245		
13	Ga3	5.300	5.3081	121	5.2977	224		
14	Ge3	5.321			5.3142	49		
16	Ge3	5.336			5.3311	126		
18	Ge3	5.348	5.3465	76	5.3448	56		
22	Se3	5.395			5.3933	77		
24	Se3	5.410			5.403	62		
46	Ni1	5.689 <sup>a</sup>			5.690	3542	5.690	1599

47	Cu1	5.716	5.7193	87	5.719	2426	5.7189	183
48	Cu1	5.723	5.7242	134	5.724	2235	5.724	134
49	Zn1	5.748	5.7477	647	5.7473	3317	5.747	128
52	Zn1	5.756	5.7541	97	5.7534	1456	5.7538	72
53	Zn1	5.765	5.7678	255	5.7671	1413		
55	Ga1	5.788	5.7922	753	5.7925	2345	5.7924	53
56	Ga1	5.791	5.7950	423	5.7952	1120		
57	Ge1	5.821	5.8315	143	5.8299	138		
58	Ge1	5.827	5.8378	515	5.8377	512		
59	Ge1	5.836	5.8465	156	5.8467	83		
60	As1	5.862	5.8552	277	5.855	148		
61	Ni2	5.870 <sup>a</sup>			5.867	1283	5.867	657
62	Se1	5.894	5.894	247	5.8927	649		
63	Cu2	5.905	5.9169	61	5.9129	808	5.9128	93

Table 2 (continued)

N	Ion Group	Theor. $\lambda$ (Å)	3.9 keV		4.0 keV		4.1 keV	
			Exp. $\lambda$ (Å)	Int.	Exp. $\lambda$ (Å)	Int.	Exp. $\lambda$ (Å)	Int.
7	Ni3	5.201 <sup>a</sup>	5.1944	789	5.1974	127	5.1969	483
8	Cu3	5.230	5.2264	67			5.2259	51
9	Cu3	5.241	5.2338	106				
11	Ni3	5.255	5.2518	146	5.2514	26	5.2511	62
12	Zn3	5.280	5.2727	57				
13	Ga3	5.300	5.2988	97				
14	Ge3	5.321	5.3126	37				
24	Se3	5.410	5.4053	42				
36	Co1	5.558					5.5646	385
37	Co1	5.563	5.5684	109	5.5705	36	5.5688	586
39	Co1	5.577	5.5812	58			5.5808	286
41	Fe2	5.608					5.6101	94
43	Fe2	5.626					5.6277	66
44	Fe2	5.630					5.6355	24
46	Ni1	5.689 <sup>a</sup>	5.690	11162	5.690	1476	5.690	6418
47	Cu1	5.716	5.7189	655	5.7184	10	5.7186	320
48	Cu1	5.723	5.7241	703	5.724	78	5.7238	428

49	Zn1	5.748	5.7467	427	5.7467	54		
50	Co2	5.745					5.7476	471
51	Co2	5.753					5.7531	291
52	Zn1	5.756	5.7535	459	5.7534	43		
53	Zn1	5.765	5.7678	44				
54	Co2	5.774					5.7743	147
55	Ga1	5.790	5.7933	169	5.7935	18		
61	Ni2	5.870 <sup>a</sup>	5.866	4660	5.866	605	5.866	2583
62	Se1	5.894	5.8921	85	5.8943	18	5.8924	34
63	Cu2	5.905	5.9127	364	5.9105	59	5.9125	196

Table 2 (continued)

N	Ion Group	Theor. $\lambda$ (Å)	4.2 keV		4.3 keV	
			Exp. $\lambda$ (Å)	Int.	Exp. $\lambda$ (Å)	Int.
2	Fe3	5.081			5.0842	88
3	Fe3	5.096			5.0901	53
4	Co3	5.114	5.1089	25		
5	Co3	5.124	5.1211	71	5.1219	45
6	Co3	5.136	5.1375	78	5.1379	92
7	Ni3	5.201 <sup>a</sup>	5.1978	323	5.1962	172
8	Cu3	5.230	5.2269	25		
9	Cu3	5.241	5.2382	36		
11	Ni3	5.255	5.2512	33		
19	Mn1	5.339	5.3443	31	5.344	80
25	Fe1	5.441	5.4495	96		
26	Fe1	5.447	5.4532	266	5.4513	408
27	Fe1	5.451	5.4581	150	5.4551	316
28	Fe1	5.458			5.4584	186
29	Fe1	5.467	5.4632	67	5.4632	94
30	Fe1	5.477			5.471	44
32	Mn2	5.505	5.5114	43	5.5103	80
34	Mn2	5.527			5.535	49
36	Co1	5.558	5.5639	772	5.5647	524
37	Co1	5.563	5.5681	1620	5.5686	850
38	Co1	5.566	5.5708	455	5.5721	253
39	Co1	5.577	5.5809	641	5.5815	402
41	Fe2	5.609	5.6099	247	5.6107	142
42	Fe2	5.615	5.6183	161	5.6181	169
43	Fe2	5.626	5.6284	102	5.6299	177
44	Fe2	5.630	5.633	123	5.6345	150

45	Fe2	5.636	5.6379	38	5.639	57
46	Ni1	5.689 <sup>a</sup>	5.690	6160	5.691	2526
47	Cu1	5.716	5.7194	311	5.720	76
48	Co2	5.726	5.724	440	5.7246	248
50	Co2	5.745	5.7479	760	5.7492	489
51	Co2	5.753	5.7529	672	5.754	318
54	Co2	5.774	5.7741	325	5.776	185
61	Ni2	5.870 <sup>a</sup>	5.866	2445	5.868	1046
62	Se1	5.894	5.8917	31		
63	Cu2	5.905	5.9116	203	5.9128	98

Table 2 (continued)

N	Ion Group	Theor. $\lambda$ (Å)	4.4 keV		4.5 keV		4.6 keV	
			Exp. $\lambda$ (Å)	Int.	Exp. $\lambda$ (Å)	Int.	Exp. $\lambda$ (Å)	Int.
1	Fe3	5.065	5.0677	52	5.0696	54		
2	Fe3	5.081	5.0857	74	5.089	124	5.088	84
3	Fe3	5.096	5.0902	72				
4	Co3	5.114			5.1106	43		
5	Co3	5.125	5.1232	65			5.1257	73
6	Co3	5.136	5.1393	74	5.1389	61		
7	Ni3	5.201 <sup>a</sup>	5.1959	241	5.1959	109	5.1960	102
10	Cr1	5.238			5.2371	47	5.236	276
15	Mn1	5.324			5.3239	13	5.3236	46
17	Mn1	5.335	5.3416	153	5.3427	561	5.3406	259
19	Mn1	5.339	5.345	252	5.3467	262	5.3448	844
20	Mn1	5.345	5.3496	70	5.3526	147	5.3508	284
21	Cr2	5.387			5.3799	39	5.3801	132
23	Cr2	5.403			5.3992	26	5.3997	89
25	Fe1	5.441	5.4486	75	5.449	111		
26	Fe1	5.447	5.4521	597	5.4526	739	5.452	691
27	Fe1	5.451	5.456	410	5.4577	644	5.4563	770
28	Fe1	5.458	5.4595	457				
29	Fe1	5.467	5.4644	39	5.4646	115	5.4667	65
30	Fe1	5.477	5.4688	52	5.4715	58	5.4726	90
31	Mn2	5.494	5.5063	85	5.504	56	5.505	184
32	Mn2	5.505	5.5124	150	5.512	275	5.511	234
33	Mn2	5.522	5.5277	36	5.5281	73		
34	Mn2	5.527	5.534	58	5.5346	140	5.5339	227
35	Mn2	5.537	5.5455	71	5.5443	124	5.5458	245
36	Co1	5.558	5.5646	525	5.5634	268	5.5635	279
37	Co1	5.563	5.5682	963	5.5677	825	5.5683	946

38	Co1	5.566	5.5714	242	5.5713	227	5.5709	116
39	Co1	5.577	5.5811	357	5.5809	292	5.5815	299
40	Fe2	5.597	5.5934	48	5.5949	52	5.5977	87
41	Fe2	5.609	5.6107	118	5.6105	140	5.6104	92
42	Fe2	5.615	5.618	272	5.6168	178	5.6174	369
43	Fe2	5.626	5.6297	234	5.6297	185	5.6305	375
44	Fe2	5.630	5.6335	165	5.6351	198	5.6361	198
45	Fe2	5.636	5.6375	141			5.6395	39
46	Ni1	5.689 <sup>a</sup>	5.690	2071	5.690	1310	5.690	1046
47	Cu1	5.716	5.719	81	5.7202	113		
48	Co2	5.726	5.7242	243	5.7251	93	5.7234	217

Table 2 (continued)

N	Ion Group	Theor. $\lambda$ (Å)	4.4 keV		4.5 keV		4.6 keV	
			Exp. $\lambda$ (Å)	Int.	Exp. $\lambda$ (Å)	Int.	Exp. $\lambda$ (Å)	Int.
50	Co2	5.745	5.7483	568	5.748	291	5.7479	236
51	Co2	5.753	5.7534	224	5.7526	243	5.7534	229
54	Co2	5.774	5.7744	179	5.7747	106	5.7746	125
61	Ni2	5.870 <sup>a</sup>	5.867	797	5.866	605	5.866	504
63	Cu2	5.905	5.9117	57				



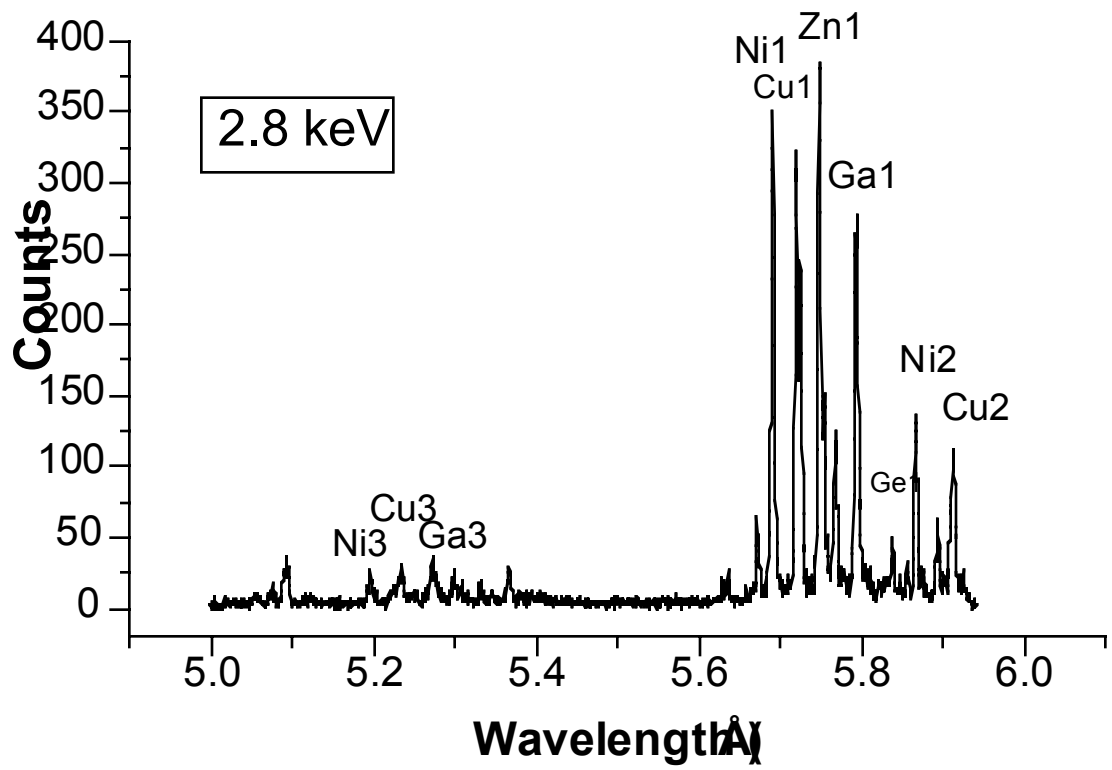
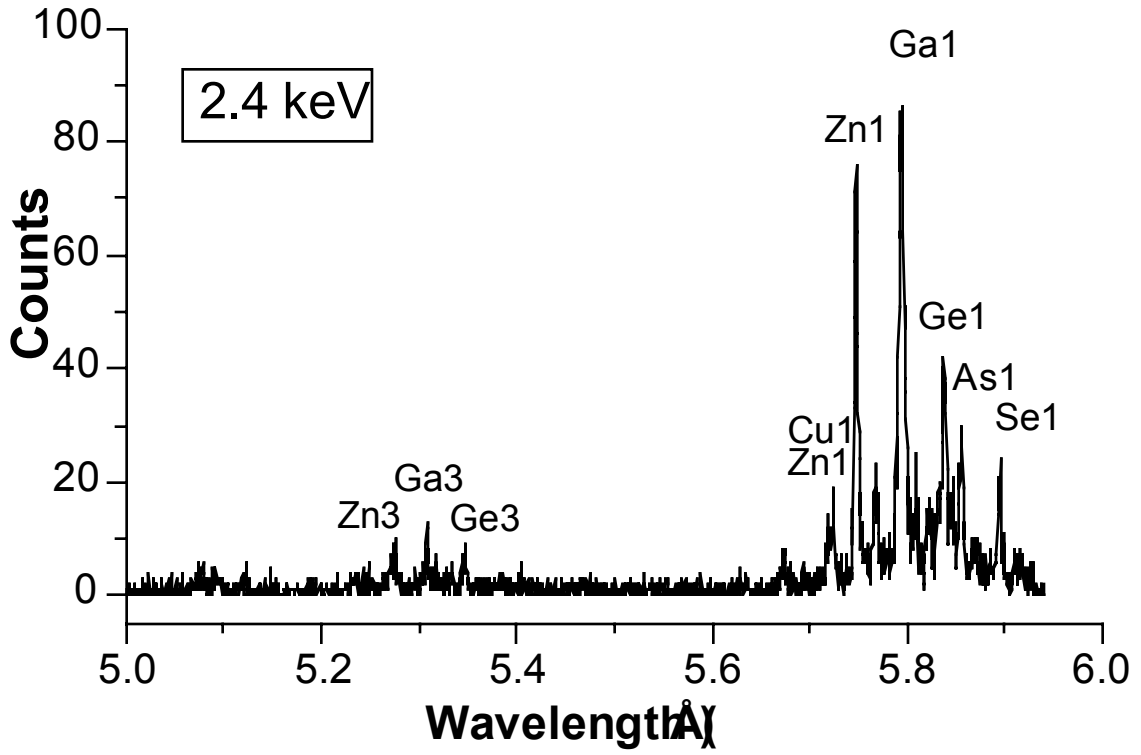


Fig. 1

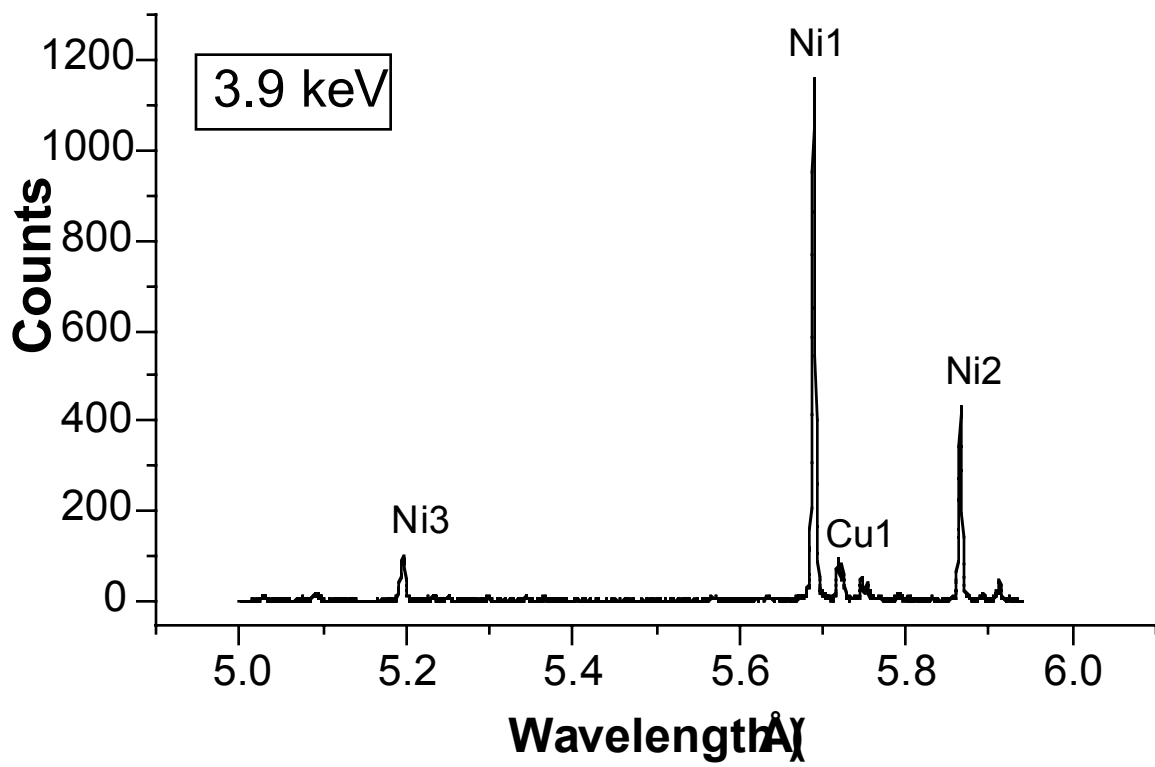
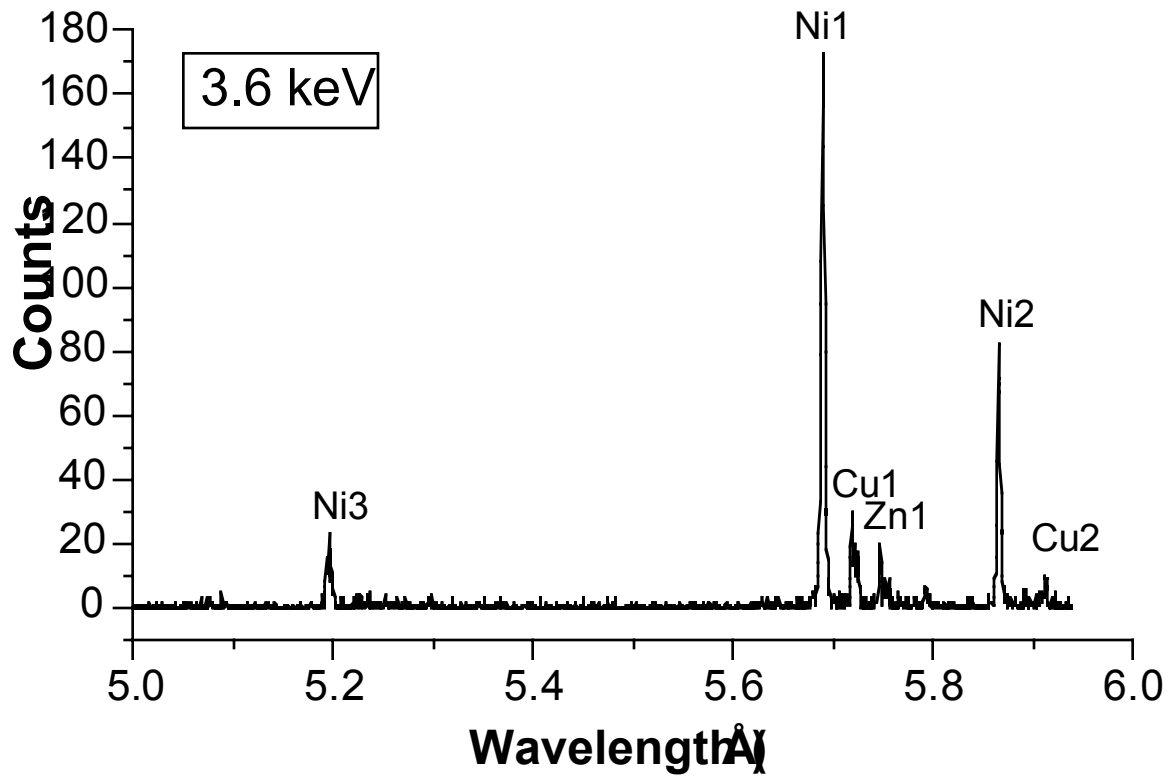


Fig. 2

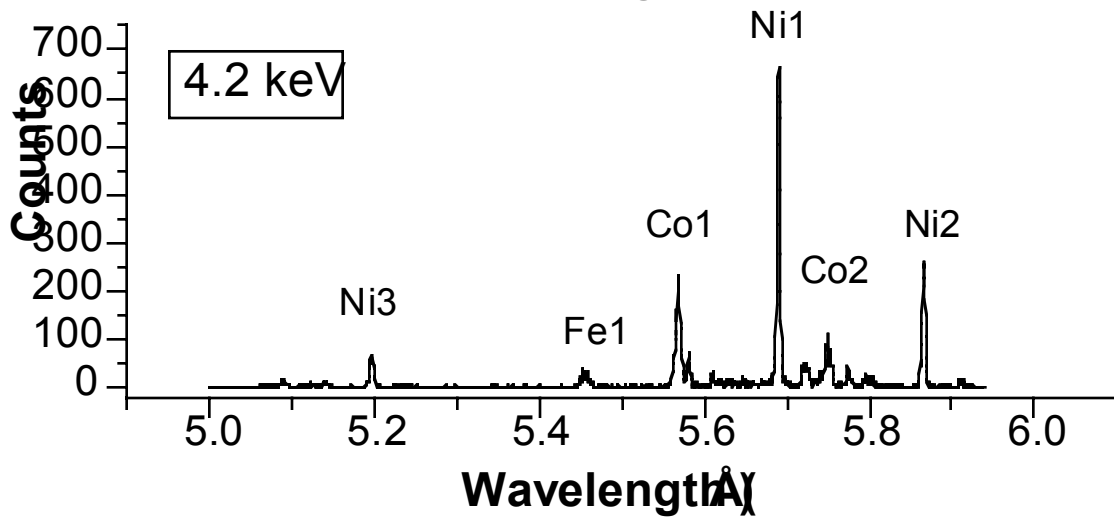
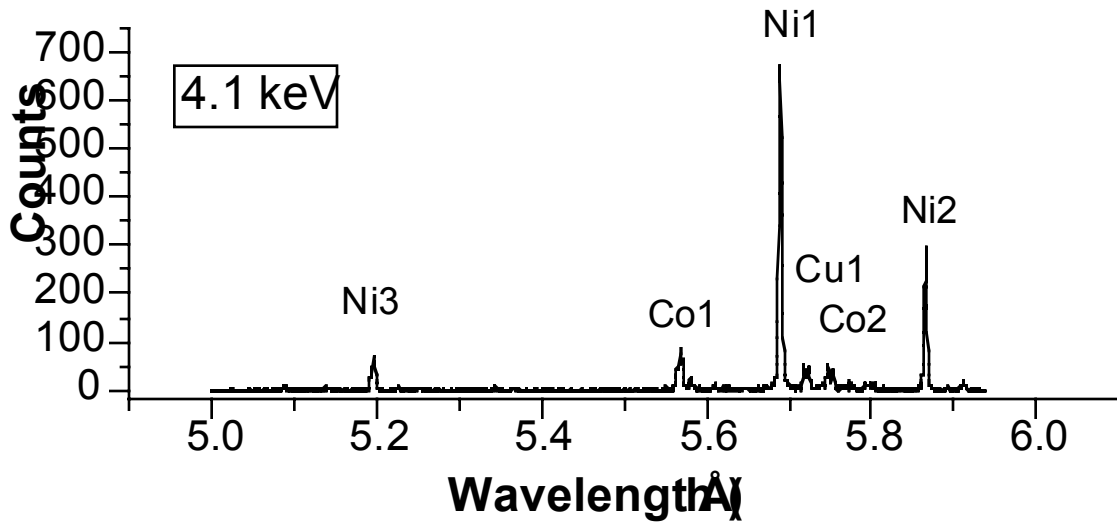
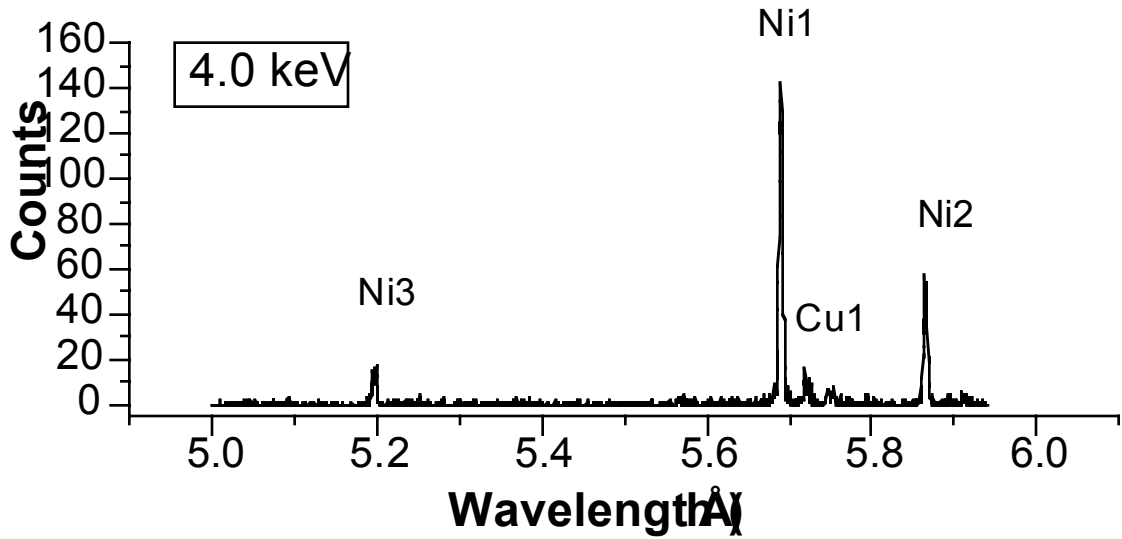


Fig. 3

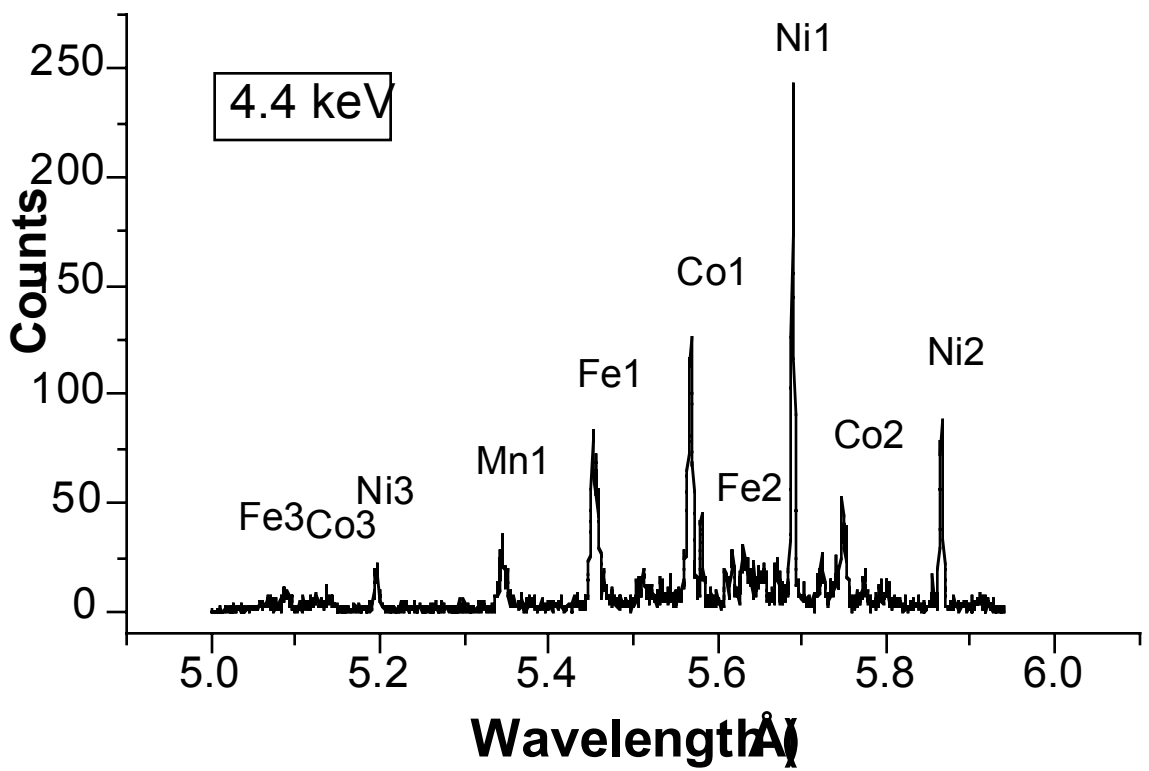
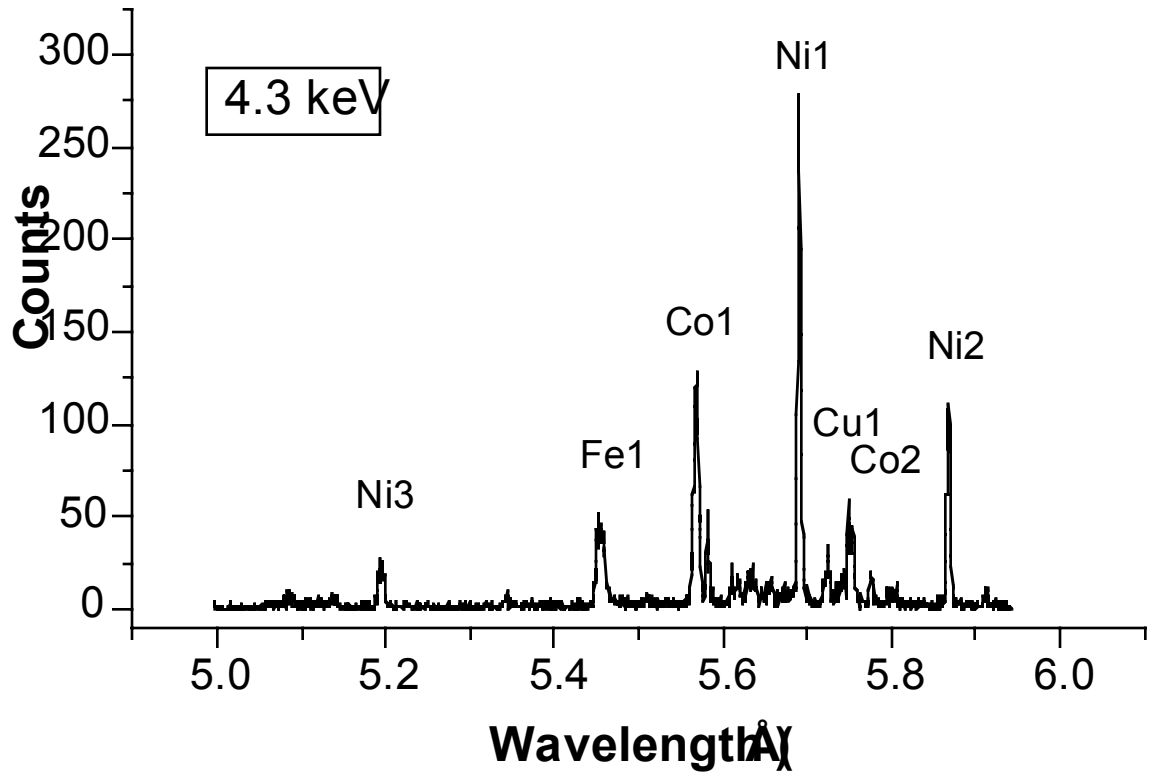


Fig. 4

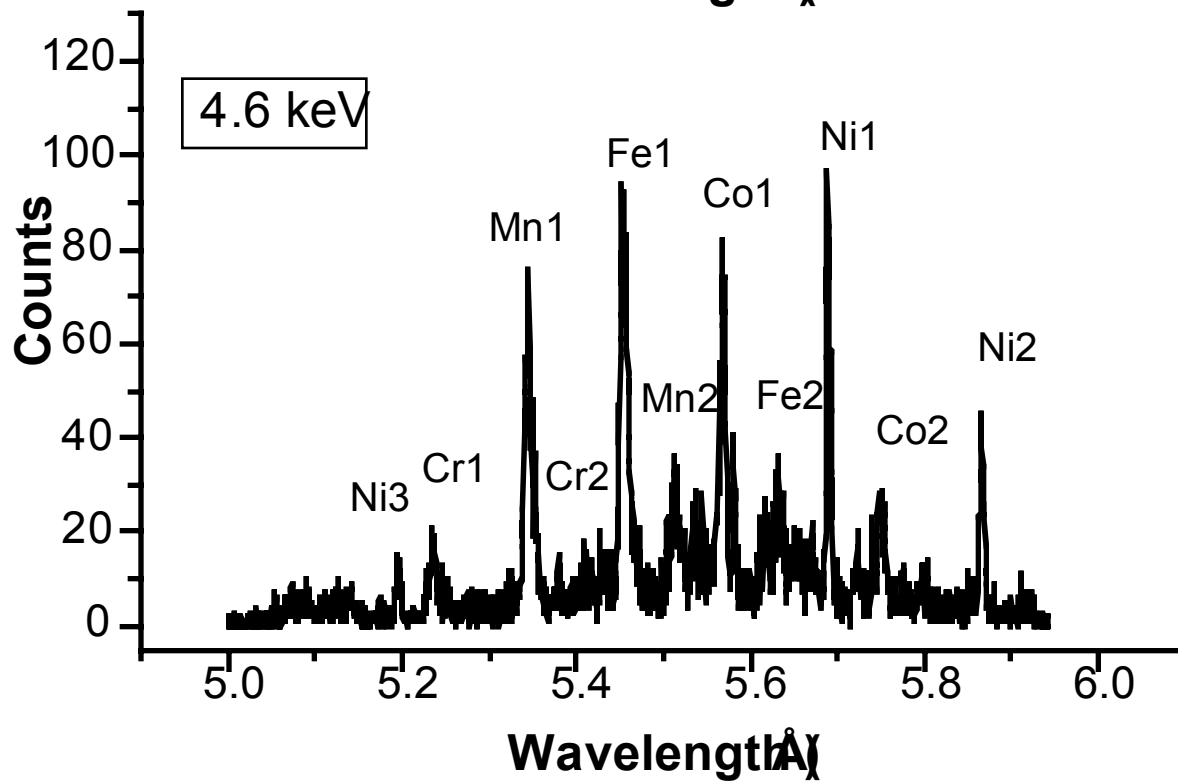
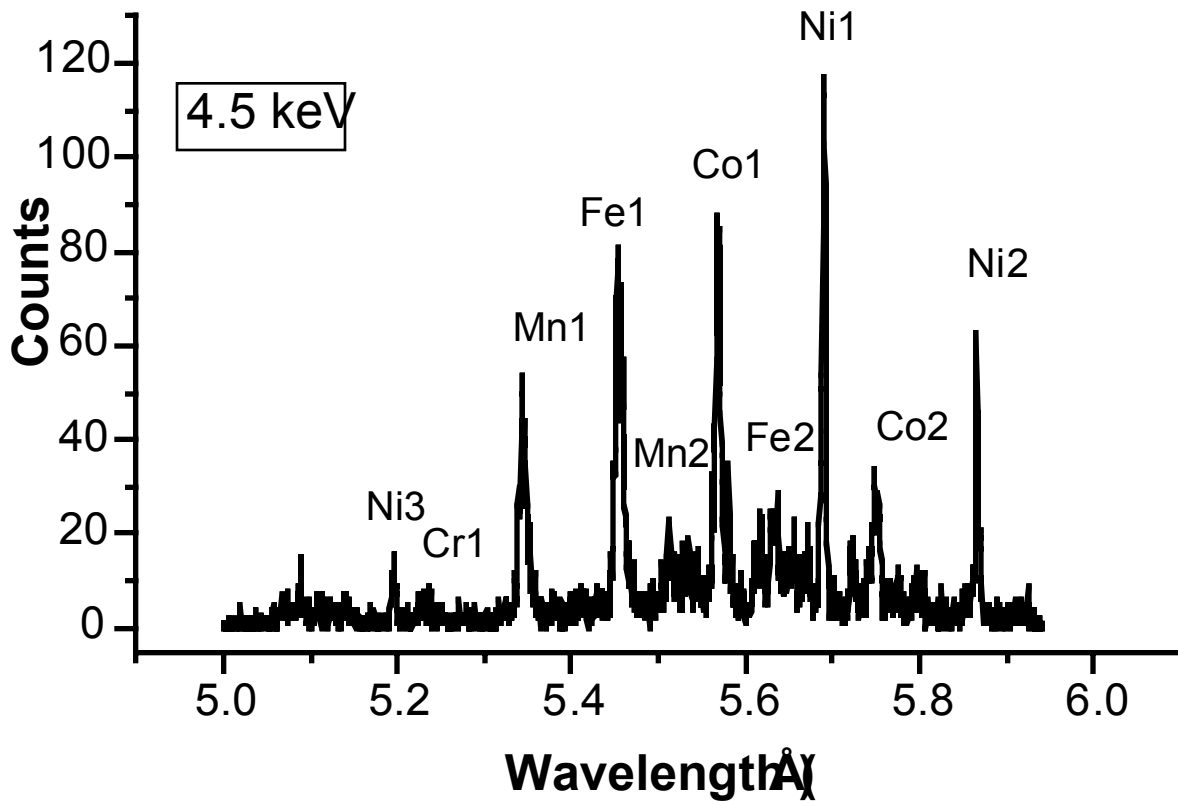


Fig. 5

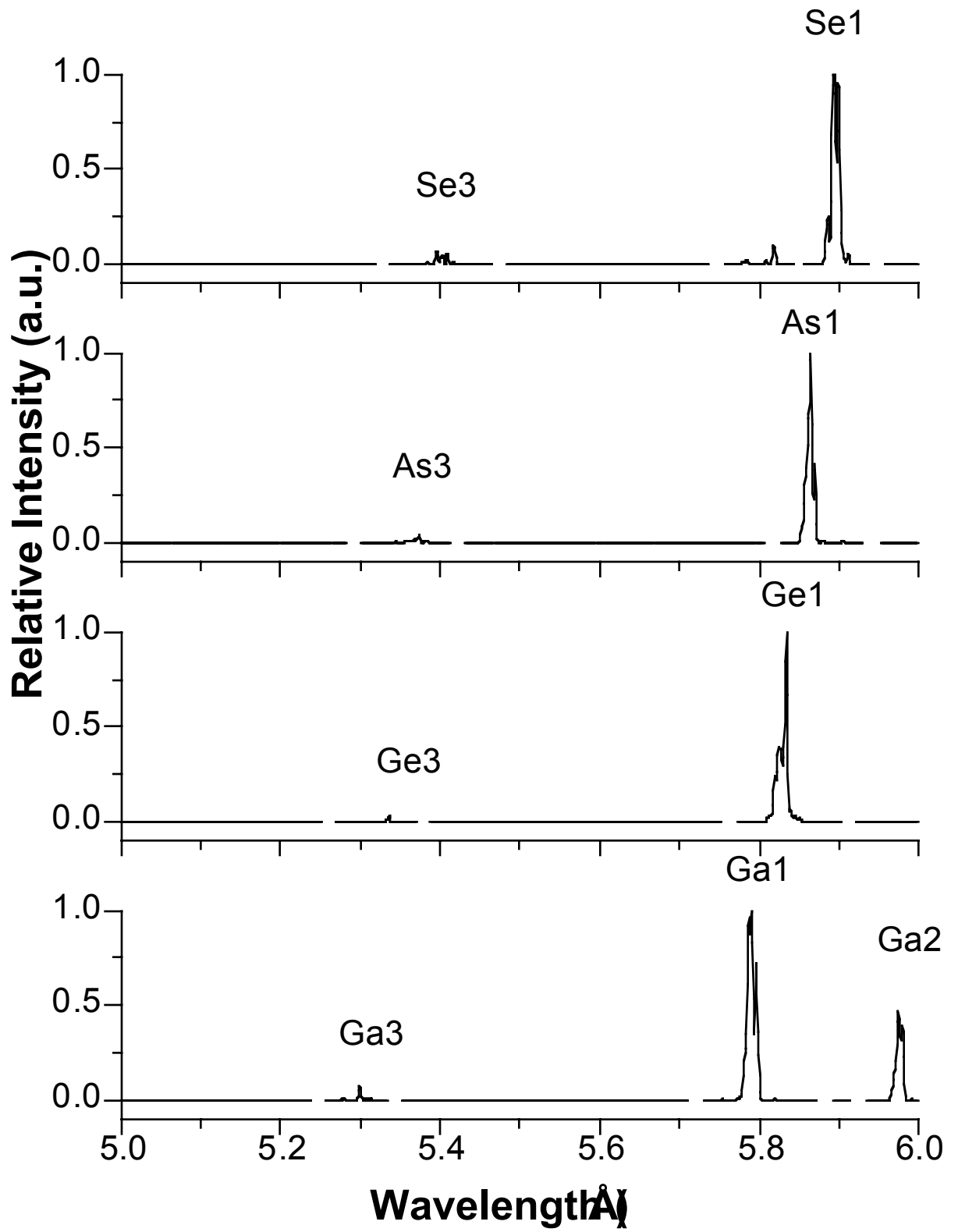


Fig. 6a

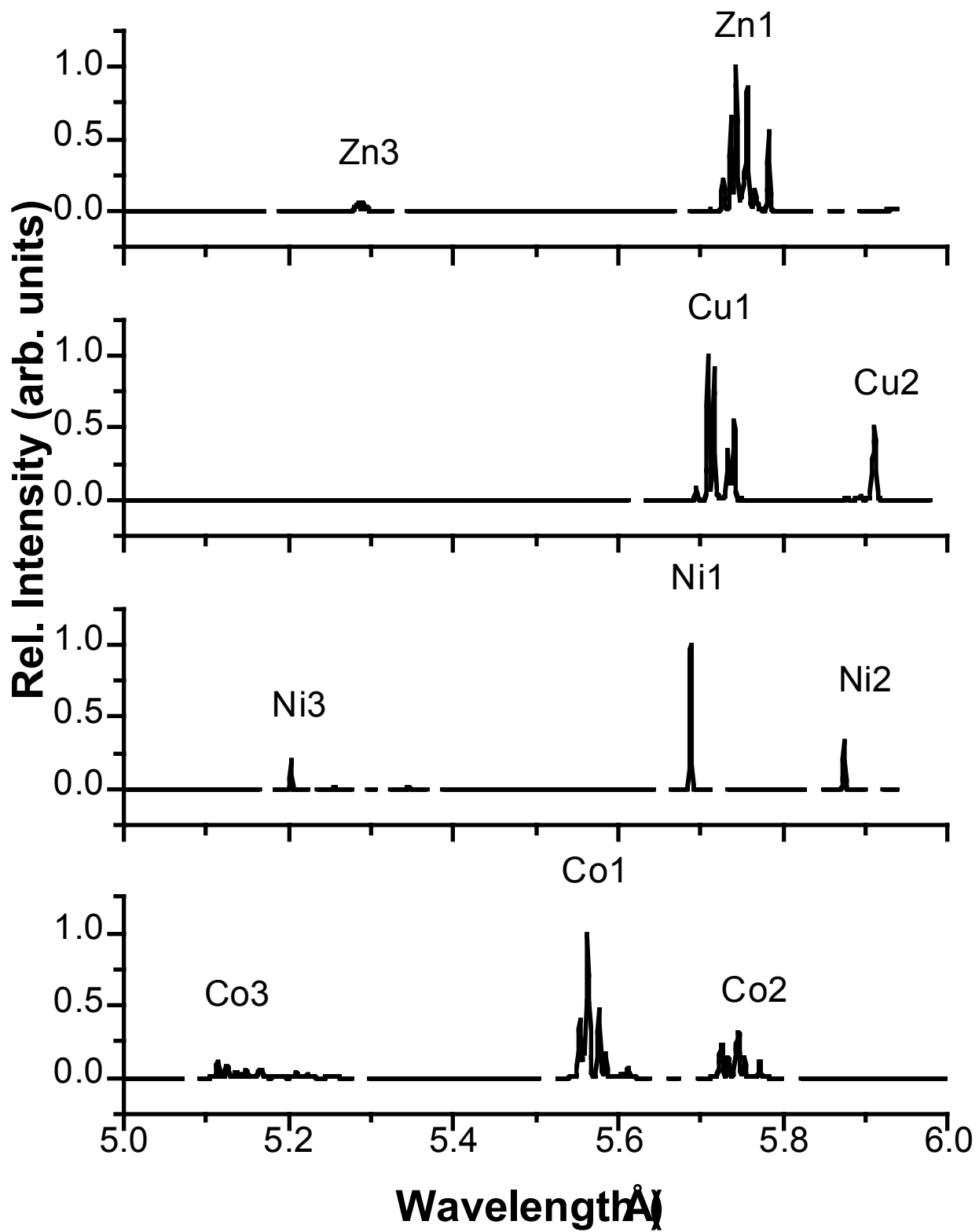


Fig. 6b

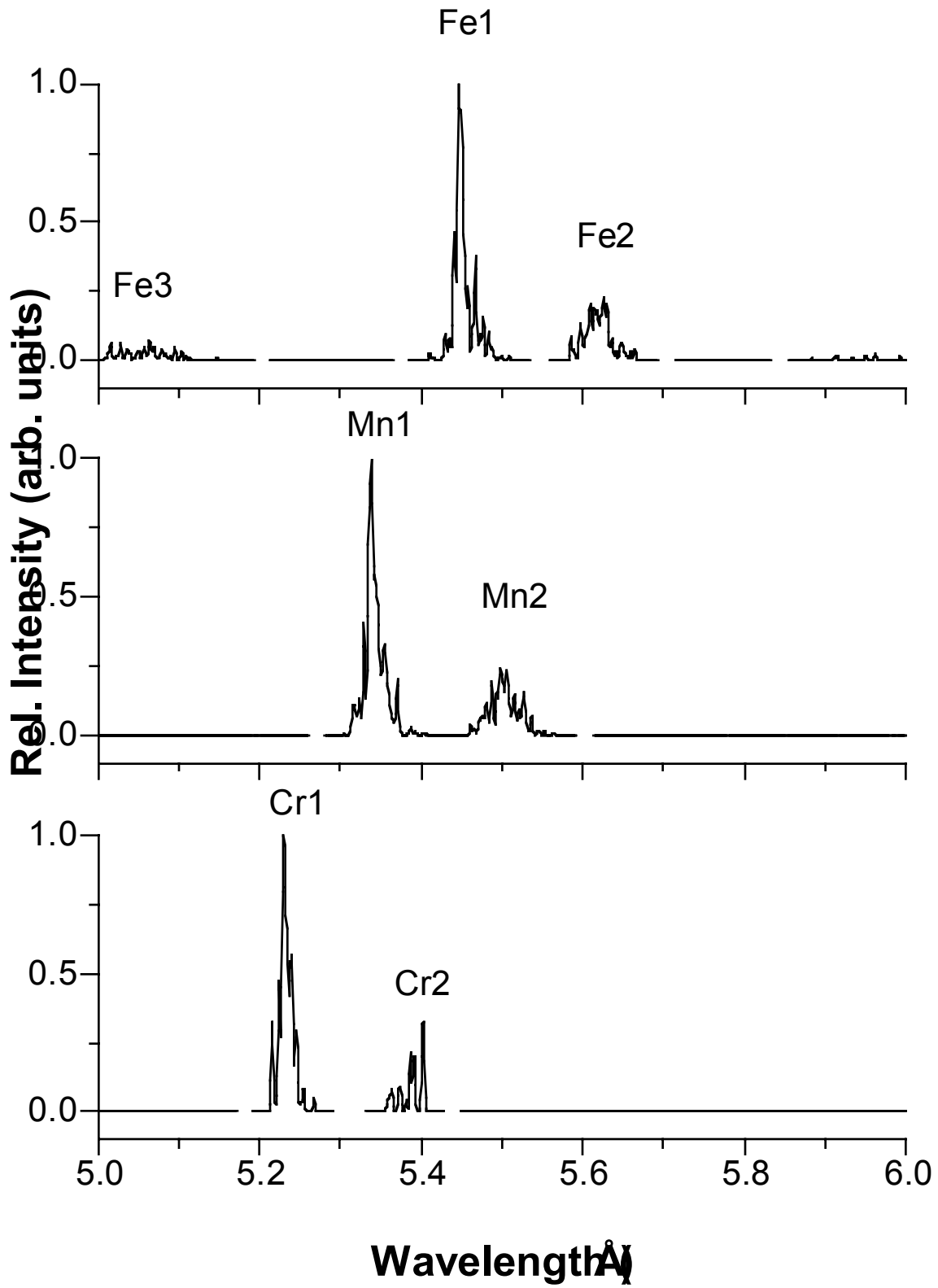


Fig. 6c

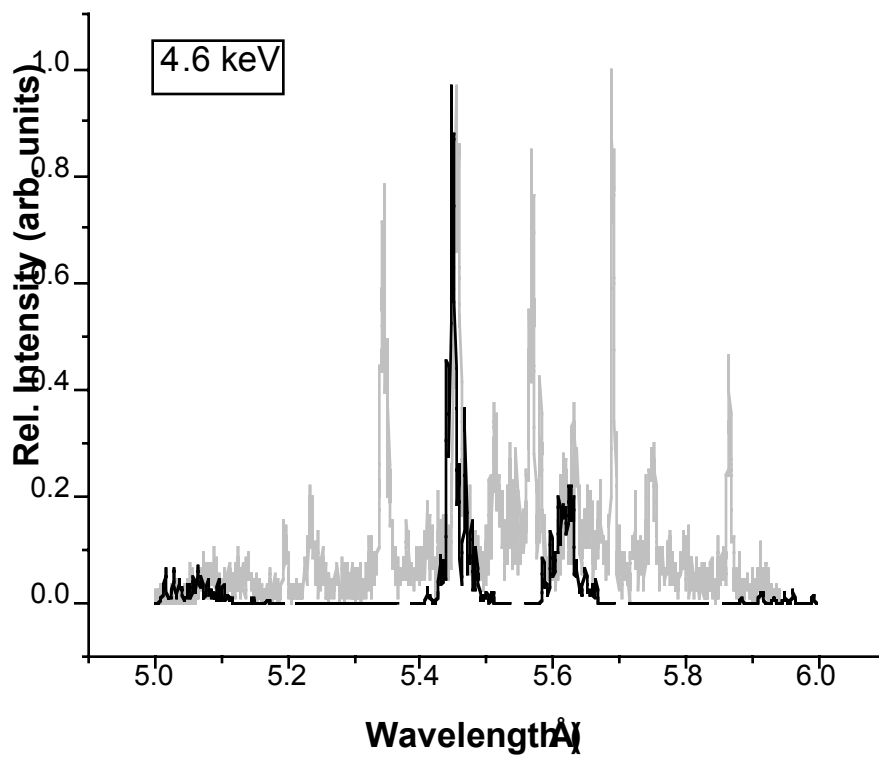
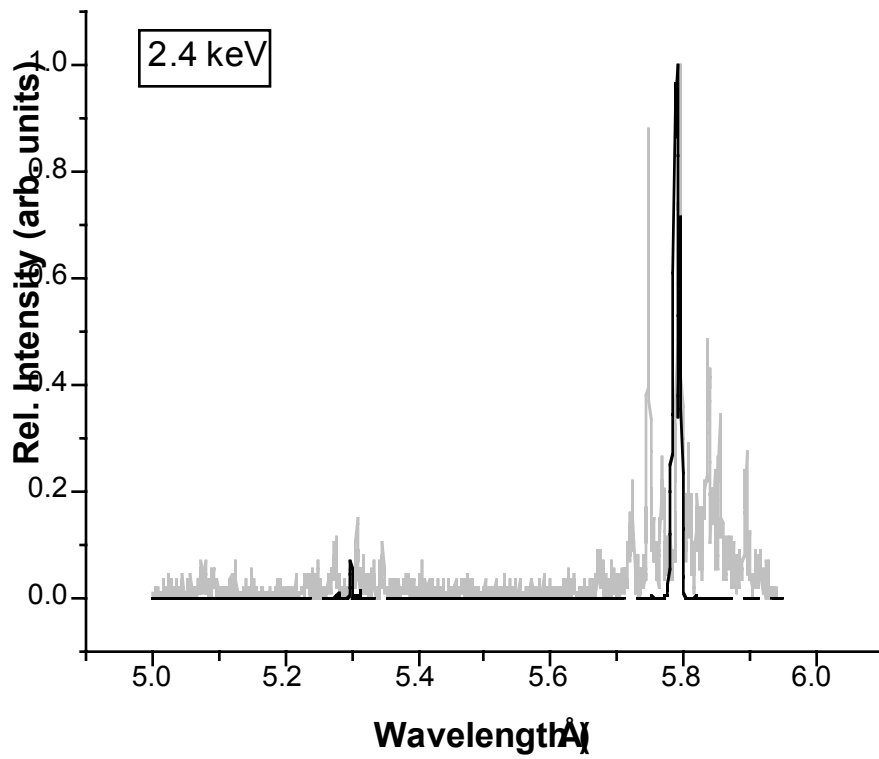


Fig. 7

University of California  
Lawrence Livermore National Laboratory  
Technical Information Department  
Livermore, CA 94551

